

IDENTIFICATION OF PHENOTYPES SUITABLE FOR DRUG TESTING IN A GENETIC OR TOXIN-INDUCED MODEL OF PARKINSON'S DISEASE USING HUMAN IPSC-DERIVED DOPAMINERGIC NEURONS.



Erika Torchio, Teresa Ferraro, Elisa Bianchini, Alessandra Toti, Andrea Kuan Cie Wong, Cristiana Griffante and Rosaria Remelli

In Vitro Pharmacology department, Aptuit (Verona) S.r.L., An Evotec Company

INTRODUCTION

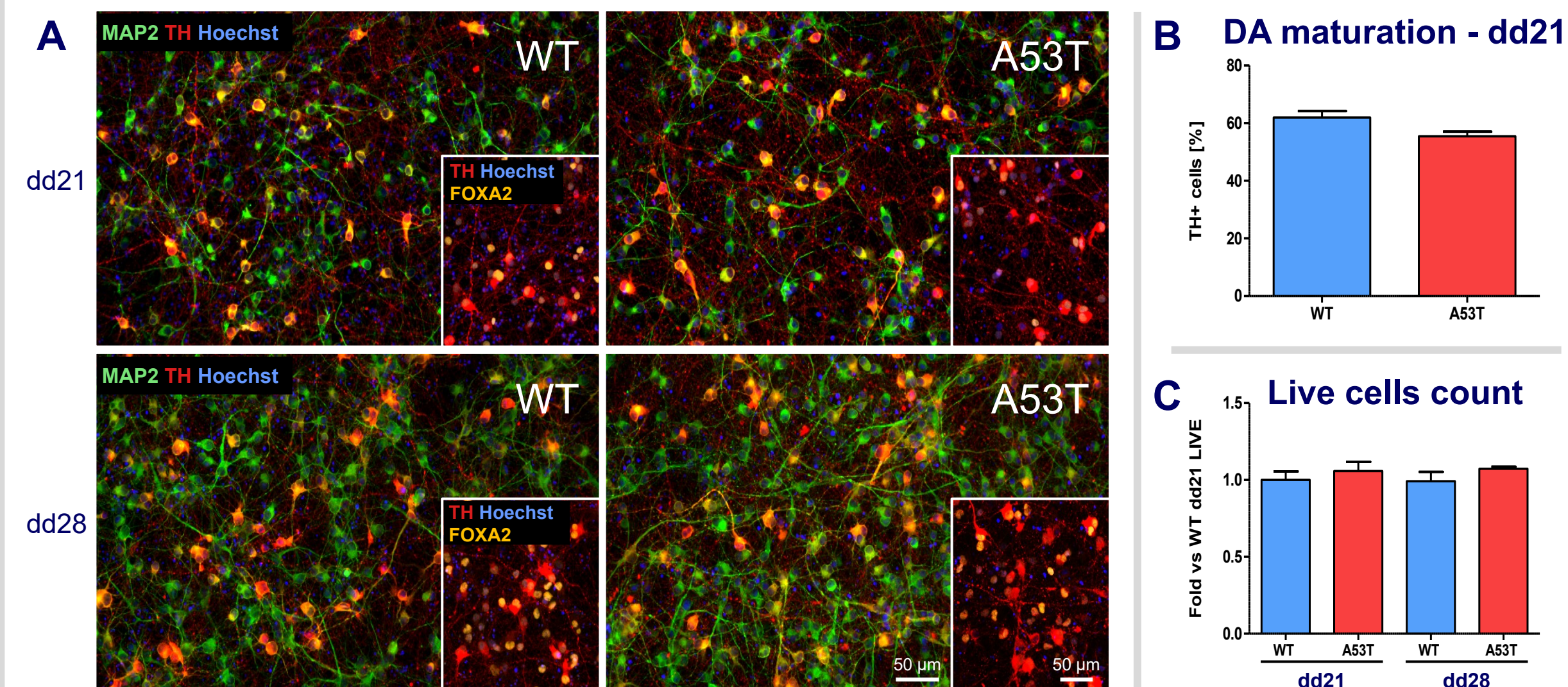
Parkinson's disease (PD) is a neurodegenerative disease caused by the progressive loss of midbrain dopaminergic neurons (mDAn). Genetic mutations affecting mDA neurons account for up to 15% of PD onsets, providing a valuable tool for studying basic pathophysiological mechanisms of the disease. One of the most relevant mutations is the A53T mutation in the SNCA gene, which causes the production of a misfolded form of alpha synuclein (αSyn), resulting in αSyn accumulation. It has been reported that PD patient neurons display a ~20% reduction of mitochondrial complex I activity. Rotenone is known to reduce mitochondrial complex I activity. Therefore testing Rotenone administration *in vitro* could mimic PD effect on mDAn mitochondria functionality.

AIM

The aim of this work is the identification of PD-relevant phenotypes for *in vitro* drug testing to be applied in drug-discovery programs for Parkinson's Disease

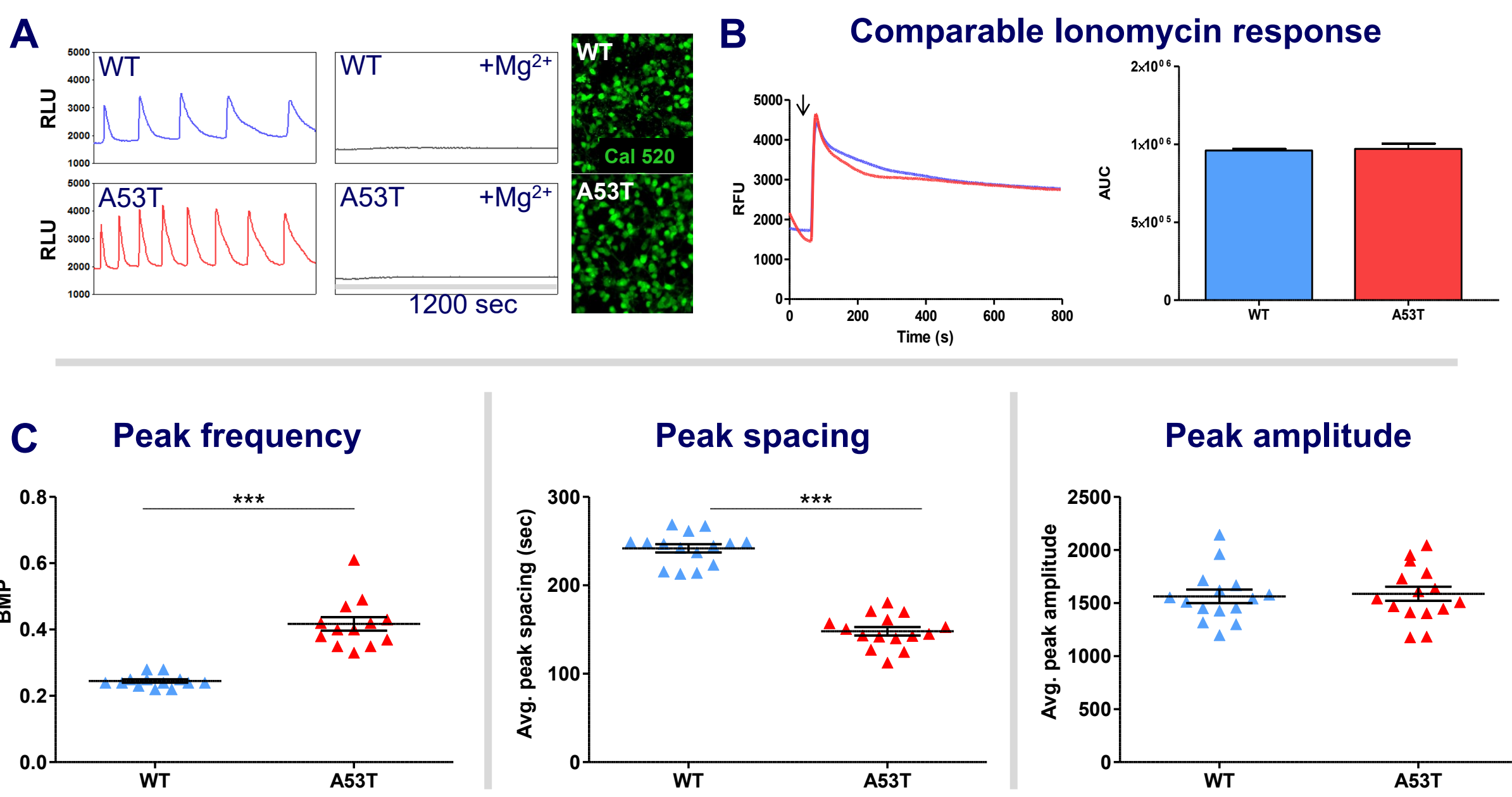
RESULTS

WT and A53T dopaminergic cultures differentiation in 384 well format



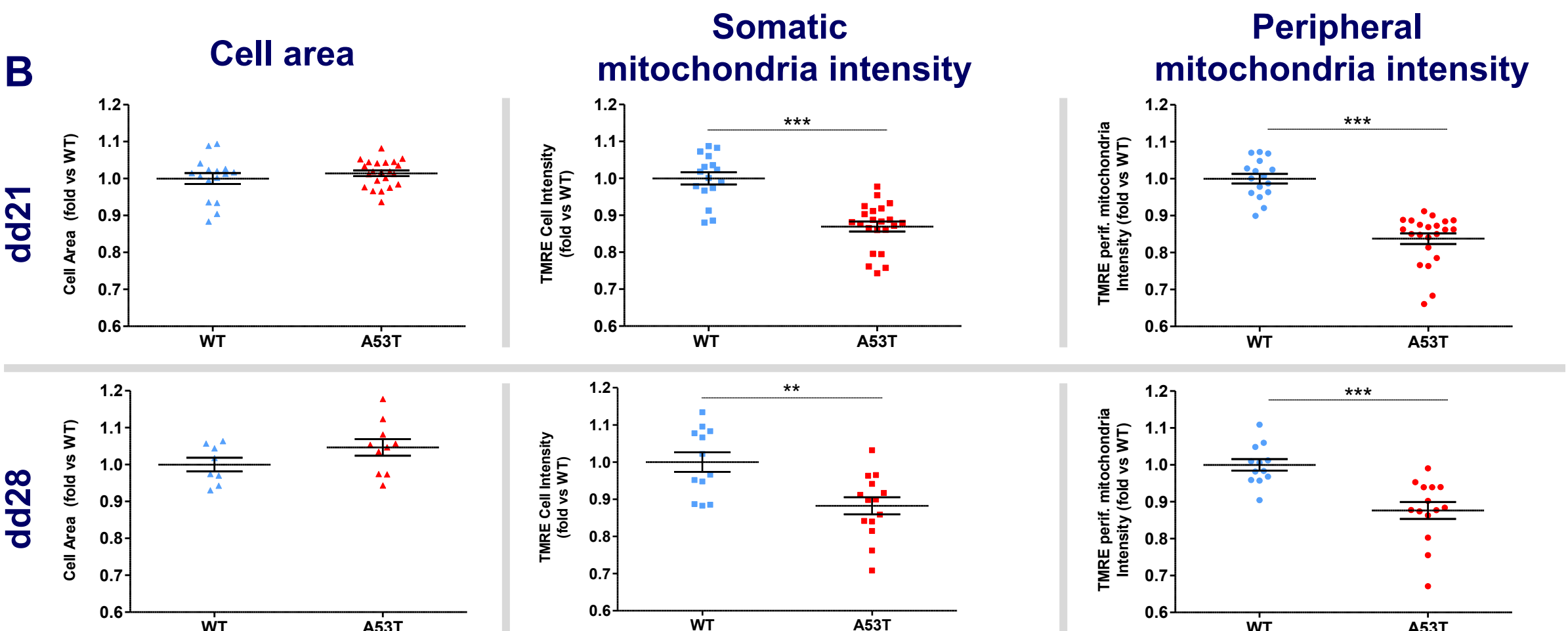
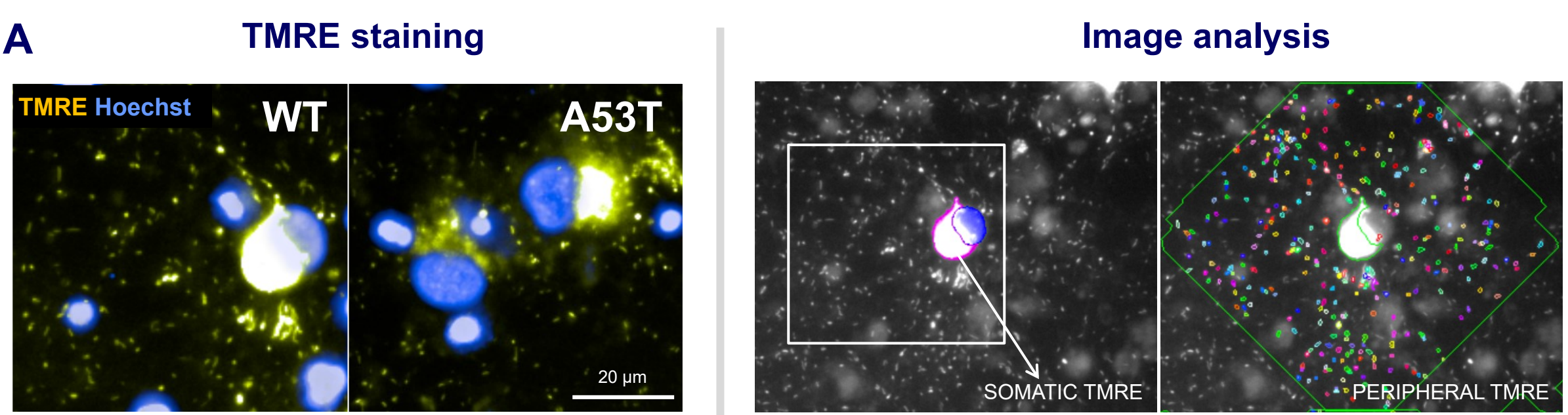
Dopaminergic neurons maturation in 384 well format: A. iPSC-derived DA-neurons maturation was confirmed by the expression of the neuronal marker MAP2 and DA-specific markers tyrosine-hydroxylase (TH) and FOXA2. B. Bar graph reports the % of TH-positive cells over live cells quantified by high content analysis (HCA). C. Viability of the cultures is quantified by HCA at dd21 and 28 by measure of the number of live c/w. Bar graph represents mean ±SEM of at least 14 replicate wells.

Different pattern of spontaneous Calcium oscillations in WT and A53T mDAn



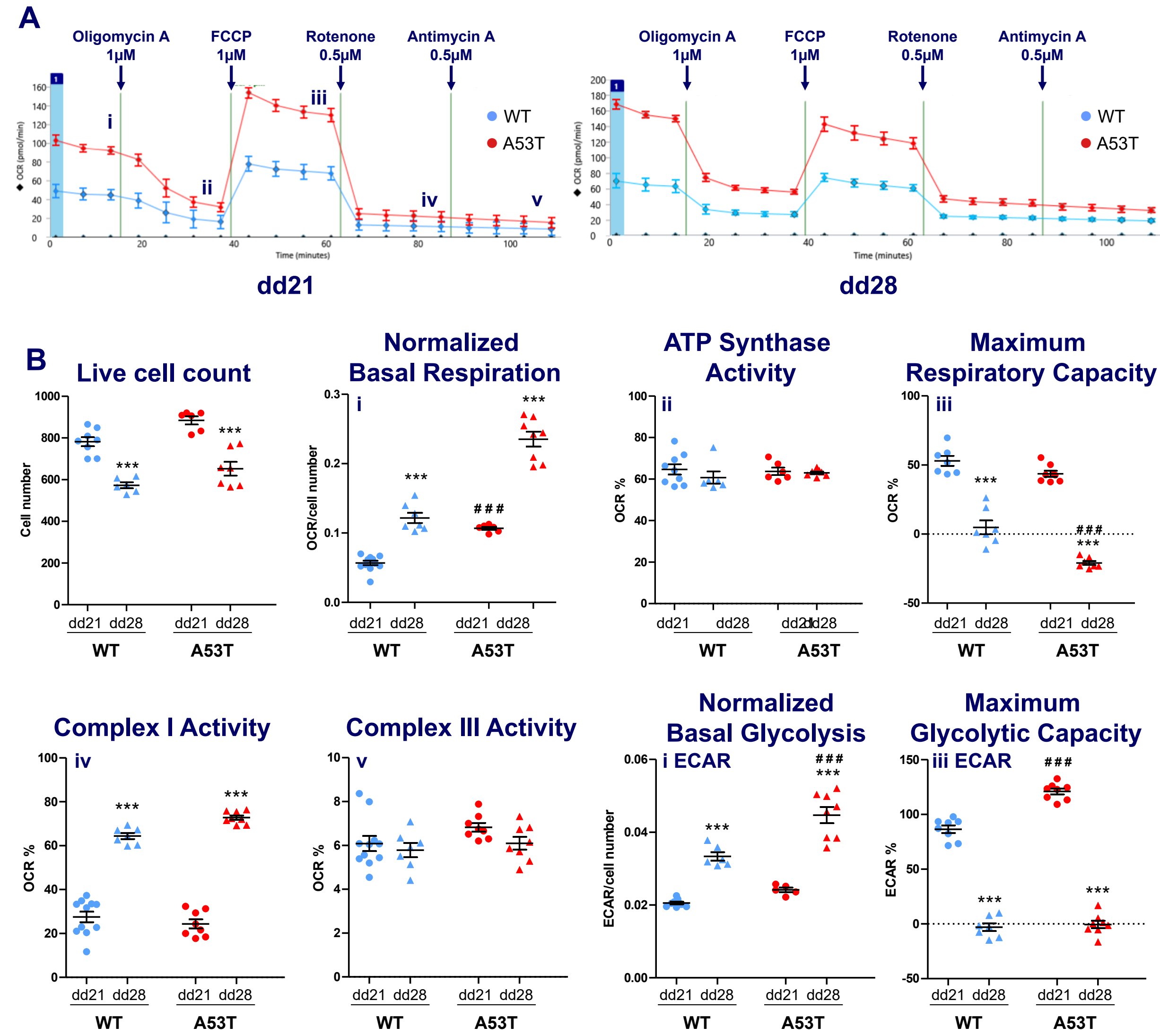
Increased frequency of Calcium oscillations in A53T DaNs compared to WT detected with FLIPR measurements in 384 well-format: Calcium oscillations with increased frequency were detected with FLIPR measurements in A53T cultures compared to WT at dd21 and dd28. A. Representative Calcium traces detected in WT and A53T mDAn. For both cultures, addition of 1μM Mg²⁺ inhibited spontaneous oscillations. Comparable cultures viability was confirmed by Cal520 staining and evaluation of the response to addition of 1μM Ionomycin (B). C. Peak analysis revealed peak frequency (BMP) 1.61 fold higher in A53T versus WT (p<0.001; t-test), 0.57 fold reduced peak spacing (p<0.001; t-test) and comparable peak amplitude. FLIPR tests performed in 4 different cultures under comparable cell viability revealed average increase of peak frequency of A53T versus WT of 1.52 ±0.1 and variable peak amplitude (fold A53T versus WT: 1.26 ±0.26).

Reduced mitochondrial membrane potential in A53T vs WT mDAn cultures



TMRE intensity quantifications performed in the cell soma and in the peripheral mitochondria showed lower Mitochondrial Membrane Potential (MMP) in A53T cultures versus WT: A. TMRE assay was performed on WT and A53T cultures at dd21 and dd28 and HCA was employed for analysis. Nuclear masks were identified based on Hoechst staining and cell masks were segmented on the TMRE signal. For peripheral mitochondria identification, TMRE spot masks were identified in the area surrounding the cells. B. Average data for each time-point from two independent cultures of WT and A53T mDAn are reported. Comparable cell area was quantified in live WT and A53T cells. TMRE intensity quantified in the cell soma of A53T displayed significantly lower signal at both time points (fold A53T vs WT: dd21, 0.87±0.01, p<0.001; dd28 0.88±0.02, p<0.01; t-test). Additionally, lower TMRE average intensity was detected in peripheral mitochondria (fold A53T vs WT: dd21, 0.84±0.01, p<0.001; dd28, 0.87±0.02, p<0.001; t-test).

Higher basal mitochondrial respiration in A53T mDAn compared to WT

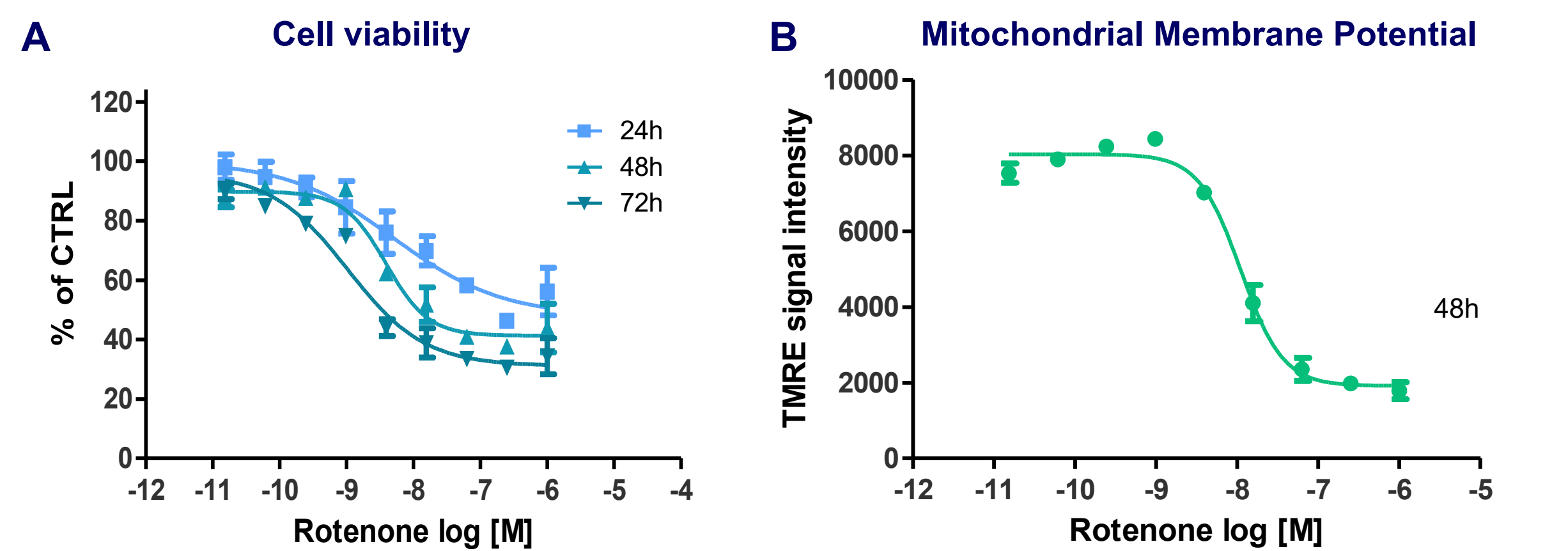


OCR (pmol/min) = oxygen consumption rate
ECAR (mpH/min) = extracellular acidification rate
ANOVA with Bonferroni post-hoc test
*** = p<0.001 (dd21 vs dd28)
= p<0.001 (WT vs A53T)

Metabolic analysis of Mitochondrial functionality of A53T and WT mDAn at dd21 and dd28 by Seahorse XF Analyzer (Agilent). A. OCR traces at dd21 and dd28 and Seahorse protocol. B. Quantification of variation of OCR (OCR %) induced by applied stimuli. Live cell number quantified by HCA (HOECHST) was used to normalize basal levels of respiration and glycolysis. Dot plot graph represents mean ±SEM.

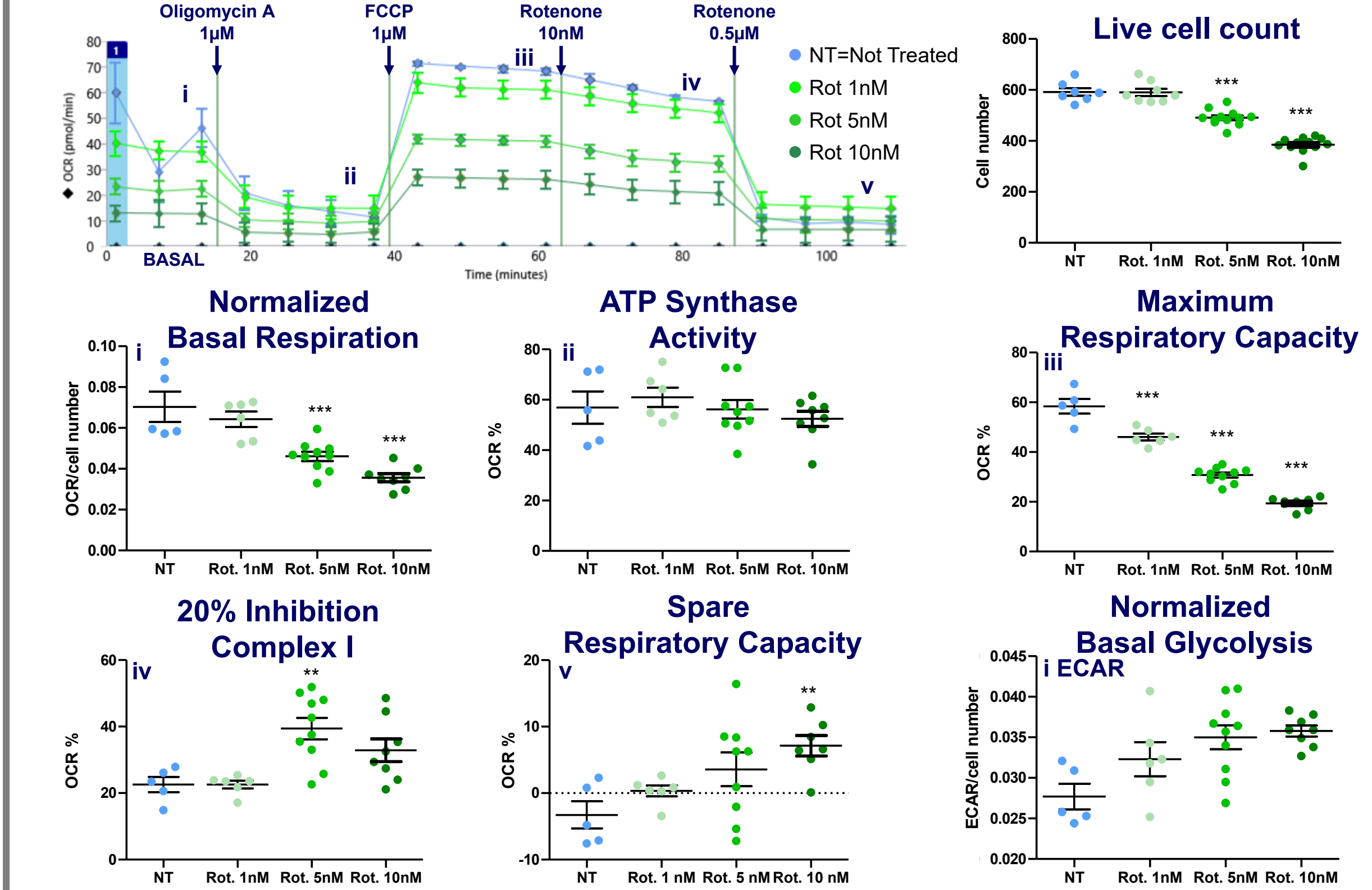
- A53T cells have higher basal respiration compared to WT mDAn (i).
- Both lines have similar response to OligomycinA (ii) and similar maximum respiratory capacity (iii), suggesting similar functionality of mitochondria in WT and A53T cells. Further studies will be performed to investigate whether the difference in basal respiration is due to differences in mitochondrial number.
- Complex I (iv) is more used than Complex III (v), which is inactive in both WT and A53T mDAn.
- Comparing dd21 with dd28, in both lines there is an increase in basal respiration (i), an increased utilization of respiratory capacity (~50% at dd21, ~100% at dd28) (iii), and a loss of glycolytic spare capacity (iii ECAR), suggesting metabolic maturation at dd28.

Acute administration of Rotenone reduces cell viability and MMP in WT mDAn



WT mDAn viability and MMP is reduced upon acute administration of Rotenone: Rotenone was administered on WT mDAn for 24, 48 or 72h. A. Rotenone reduced the cell viability in a time-dependent manner with EC₅₀ 2.3nM at both 24 and 48h, but with a maximal effect at 48h. To assess cell viability, RT-Glo luminescence were measured using CLARIOstar (BMG LABTECH). B. TMRE assay was performed on cells treated with Rotenone dilution curve after 48h of treatment. Rotenone reduced the MMP with an EC₅₀ of 9.5nM.

Chronic Rotenone administration reduces basal mitochondrial respiration



Metabolic analysis of Mitochondrial functionality of WT mDAn after chronic Rotenone treatment. WT mDAn were treated with Rotenone from dd3 to dd21 to simulate chronic inhibition of Complex I. 5 and 10nM of chronic Rotenone treatment reduced cell viability and basal respiration (i) but had no effect on ATP Synthase activity (ii). 10nM Rotenone stimulus was used to reduce Complex I activity by 20%, revealing increased cell vulnerability of cells chronically pre-treated with Rotenone (iv). To compensate chronic reduction of Complex I, mDAn adopted two strategies: induction of other mitochondrial complexes (v) and induction of glycolysis (i ECAR). Dot plot graph represents mean ±SEM, **=p<0.01, ***=p<0.001, ANOVA with Dunnett's post-hoc test.

CONCLUSIONS

In this study, an extensive phenotypic characterization of iPSC-derived mDAn cultures carrying a PD-relevant mutation (A53T) was performed in parallel to isogenic healthy control cultures (WT). Moreover, acute and chronic Rotenone administration on WT mDAn was used to induce mitochondrial stress.

Key cellular features related to PD pathogenesis were explored:

- mDAn differentiated in 384 well plates express neuronal marker MAP2 and DA-specific markers tyrosine-hydroxylase (TH) and FOXA2
- Compared to WT mDAn, an accumulation of αSyn was detected in A53T cells after 28 days in culture
- A53T mDAn display a different pattern of spontaneous Calcium oscillations compared to WT cells, potentially revealing a dysregulation of intracellular Calcium homeostasis (FLIPR 384-well assay)
- A reduced mitochondrial membrane potential was detected in A53T mDAn compared to WT cells
- A53T mDAn show higher basal respiration compared to WT in Seahorse XF metabolic assay
- Rotenone administration results in reduction of cell viability and MMP (acute treatment), as well as in reduction of mitochondrial respiration (chronic treatment). Inhibition of Complex I was compensated by induction of other mitochondrial complexes and of glycolysis.

The above mentioned assays provide a panel of readouts suitable for testing potential therapeutics acting on different PD pathophysiological mechanisms.

METHODS

mDAn cultures: iCell® DopaNeurons (WT) and MyCell® DopaNeurons (A53T) were seeded according to vendor's instruction in iCell Neural medium (Fujifilm Cellular Dynamics) on PDL/PLO/Laminin coated plates. Cells were seeded at the density of 65,000 (WT) and 50,000 (A53T) c/w for imaging studies (384w plates); at 130,000 (WT) or 100,000 (A53T) c/w (96w plates) for FLIPR and Seahorse studies. Culture medium was replaced with BrainPhys™ Neuronal Medium (StemCell Technology) after 3 days in culture and maintained for up to dd21 or dd28 with half medium volume exchange twice/week.

Immunofluorescence and Imaging: Cells were fixed in paraformaldehyde, permeabilized and incubated with primary antibodies, followed by fluorescent secondary antibodies. Primary antibodies: Ms-anti-αSyn BD-610786; Ch-anti-TH (Abcam ab76442), Rb-anti-FOXA2 (Cell Signalling 8186), Ms-anti-MAP2 (Abcam ab32454). All images were captured with InCell Analyzer 2200 and analyzed with Columbus Image Analysis System (PerkinElmer).

Mesoscale Immunoassay: Mesoscale Discovery (MSD) 96-well assay kit U-PLEX human αSyn K151WKK and GAPDH-K151PWD were used according to manufacturer instructions. For testing αSyn, 0.25μg/well was used, for GAPDH 0.125μg/well.

FLIPR Ca²⁺ assay: Cells were stained with 10μM Cal520 calcium indicator (Abcam) in Tyrode's buffer without Mg²⁺. Measurements were carried out for 20 minutes. FLIPR Screenwells® Peak Pro™ Software was used for Peak analysis.

TMRE assay: cells were incubated with 30nM TMRE (Invitrogen) for 30 minutes in culture media without phenol-red, followed by 5 minutes of incubation with HOECHST for nuclei staining.

Seahorse XF assay: Cells were pre-incubated for 1h with assay buffer before the experiment (Agilent Seahorse XF DMEM, 25mM Glucose, 2mM Glutamine, 1mM Na-Pyruvate). All stimuli were prepared as 10x solutions and added automatically by Seahorse XF instrument. 3 measurements were taken for baseline and 4 measurement were taken after every stimulus.

REFERENCES: (1) Kwon et al. 2004, DOI 10.1074/jbc.M407336200. (2) Zheng et al. 2016, DOI: 10.7554/eLife.13374